Macromolecules
ARTICLE

Macromolecules **2009**, *42*, 5881–5891 **5881**
DOI: 10.1021/ma900819b

Interaction of Particles with a Polydisperse Brush: A Self-Consistent-Field Analysis

Wiebe M. de Vos,* Frans A. M. Leermakers, Arie de Keizer, J. Mieke Kleijn, and Martien A. Cohen Stuart

Laboratory of Physical Chemistry and Colloid Science, Wageningen University, Dreijenplein 6, 6703 HB Wageningen, The Netherlands

Received April 15, 2009; Revised Manuscript Received June 11, 2009

ABSTRACT: Two complementary theoretical approaches are used to study the effect of polydispersity on (anti)fouling properties of a neutral polymer brush. Polydispersity is described using the Schulz−Zimm distribution. The Scheutjens−Fleer self-consistent-field (SF-SCF) formalism is used to consider the interaction between a single particle and a polydisperse brush with grafting density σ, focusing on the influence of the polydispersity index. The larger the polydispersity, the easier it is for a small particle (with radius $R \sim 1/(2\sqrt{\sigma})$) to penetrate the brush. Hence, the monodisperse brush is better suited to protect a surface against the adsorption of small particles compared to a corresponding polydisperse brush. The brush grafting density, however, remains the most important parameter for tuning the brush antifouling properties against small particles. For large particles (modeled as a flat wall) an opposite effect of polydispersity is found: it is harder to compress a polydisperse brush than a corresponding monodisperse brush, and thus a polydisperse brush is better suited to protect the surface against adsorption of large particles. A less-detailed approach, based on the stacking of Alexander−de Gennes boxes, is used to study the adsorption of many particles into a polydisperse brush. Consistent with the single-particle data generated by the SF-SCF theory, for weak attraction between the particles and the brush the absolute adsorbed amount remains low but increases strongly as a function of polydispersity (from $M_w/M_n = 1-2$ by a factor of 2−4). Obviously, at higher attraction between the particles and the brush the adsorption increases, but a less strong dependence on the polydispersity index is observed.

Introduction

Polymer brushes have been widely investigated over the past 30 years, for example, because of their role as particle stabilizers and their antifouling properties.[1−5] In this paper we will focus on how particles can partition into a brush. Brushes are dense layers of polymer chains end-attached to a surface. The chains are stretched in order to reduce their excluded-volume interactions. When a particle, such as a protein, is inserted into a brush, the extra excluded-volume interactions force the polymer chains to increase their stretching, causing the free energy to go up. As a reaction to this, the brush tends to push out the inserted particle. Thus, as long as there is no additional attraction between the polymer chains and the particle, the brush is potentially well suited to prevent fouling of the surface.

Antifouling properties have been investigated both experimentally[6−9] and theoretically.[8−13] Interestingly, there appears to be a remarkable disparity between theoretical and experimental investigations. In theoretical studies, the polymer brush is invariably assumed to be monodisperse; i.e., all chains have the same length. In contrast, in all experimental investigations brushes are to a significant extent polydisperse, as polydispersity is unavoidable in the production of polymer brushes.

In a recent paper de Vos and Leermakers[14] modeled polymer brushes composed of chains with a Schulz−Zimm length distribution, using a numerical self-consistent-field theory implementing the discretization scheme of Scheutjens and Fleer (SF-SCF). In that paper it was proven that even a relatively small degree of polydispersity suffices to completely destroy the parabolic density profile that is characteristic for the monodisperse brush. Increasing the polydispersity at fixed grafting density increases the average height of the brush but decreases the average stretching. The internal structure of the brush is strongly affected by polydispersity as well. Short chains are found to be compressed close to the grafting interface, whereas longer chains have a characteristic flowerlike conformation. These longer chains stretch strongly (forming a stem) when surrounded by smaller ones and decrease their stretching (forming a crown) as the density increases in the outer part of the brush. The distribution of the free ends, i.e., the end-point distribution, reflects the fluctuations in the conformations of the chains. For a monodisperse brush these fluctuations are anomalously large (proportional to the chain length) as can be concluded from the fact that the end points distribute throughout the brush. In the polydisperse brush, on the other hand, the fluctuations per chain length fraction are strongly suppressed: the distribution of ends are narrow, and the width does not depend on the length of the chain. This means that the fluctuations are small. These results might indicate that the monodisperse brush has a limited relevance for practical situations. However, when the distributions of the free ends in the polydisperse case are added together, they cover the whole brush, similarly as in the monodisperse brush. The latter may explain why the monodisperse brush has been so successfully applied to experimental situations. Nevertheless, to date there is, as far as we are aware, no knowledge about the effects of polydispersity on the (anti)fouling performance of a brush.

At the turn of the century a theoretical approach to investigate the interaction between a polymer brush and a single particle was

*To whom correspondence should be addressed.

Published on Web 06/26/2009

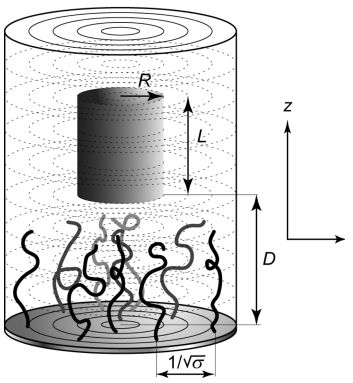

Figure 1. Schematic representation of the coordinate system used in the SF-SCF calculations. Here we show a small particle (top gray cylinder) with radius R and height L positioned at a distance D from the substrate. The two-gradient coordinate system (z,r) is indicated; layers parallel to the surface are numbered $z = 1, 2, ..., M_z$. In radial directions the lattice shells are numbered $r = 1, 2, ..., M_r$. At the surface, a polymer brush with grafting density σ is present. In the SCF model we assume that the brush chains are laterally mobile along the surface. To avoid adverse effects of the finite size of the computation box, the boundary condition in the radial direction is mirror-like.

devised by Steels et al.[13] They used a two-gradient numerical self-consistent-field theory (also using the SF-SCF approximations) to investigate the changes in the brush density profile upon the insertion of a cylindrical object (with length L and radius R; see Figure 1). They were able to compute the interaction (free) energy between such a particle and the brush as a function of the position of the particle above the grafting surface, for different grafting densities and particle sizes. The authors showed that the size of the particle is very important for the way it interacts with the polymer brush. While a relatively small particle (compared to the distance between the grafted chains) is able to penetrate the brush layer, a larger particle can only compress the polymer chains in the brush.

We extend the study of Steels et al.[13] to account for the polydispersity of the polymer chains that form the brush and use numerical self-consistent-field theory to determine the interaction energy between a single particle and a polydisperse brush. For the polydispersity, the relevant case of the Schulz−Zimm distribution is used. We consider (i) a very small particle penetrating the brush and (ii) a large particle compressing the brush. For both limits we investigate (a) systems where only excluded-volume interaction are important, (b) systems with a weak attraction between the brush and a particle, and (c) systems with a large attraction between the brush and a particle. We note that in the intermediate (mesoscopic) regime of particle sizes the details of how the polydispersity of the grafted chains is handled (the grafting position is quenched or annealed) are important. In this paper, however, such details are avoided mostly for computational reasons.

In practice, one is interested in the number of particles per unit area that accumulate into the brush at a given particle concentration in the (bulk) solution. Such information typically is collected in adsorption isotherms. Of course, when there is sufficient repulsion, the adsorption is negligible (or in fact negative), but when attractive interactions are turned on, the adsorption can grow to relatively large values. The SF-SCF approach can account for many details of how the polymer chains accommodate a single particle. In addition, the method allows for the evaluation of the free energy of interaction of a particle with the brush (as mentioned above). This insertion free energy can be used in a Boltzmann equation to estimate the distribution of the particles in the brush. Integrating over this distribution leads to the Henri coefficient (initial rise of the adsorption at very low levels of loading) of the adsorption isotherm. For large adsorbed amounts, however, one has to consider how multiple particles disturb the brush. This problem is currently out of reach for molecularly detailed SCF models. To circumvent this problem and estimate the adsorption isotherms, we will use a less rigorous SCF approach known as the Alexander−de Gennes box model, which we extend to account for polydispersity in a reasonable way. A similar box model, in the absence of particles, has been applied to the polydisperse brush in ref 14. Using this model, we will investigate how polydispersity of the brush influences the adsorption of multiple small particles.

In both the SCF method and in the Alexander−de Gennes box model, we can identify the transition point that separates the adsorption from the depletion regime. So, in first order we can bring both approaches together so that they complement each other. However, as the two methods treat the particle-insertion problem on a different level of detail, it is hard to match them accurately. It is not the goal of this paper to determine what values for the pertinent parameters in each approach should be used to describe a particular experimental system. Instead, we will focus on how polydispersity of the brush influences the uptake or repulsion of particles. In other words, we are here interested in predicting (measurable) trends rather than to make a quantitative comparison to experiments.

Theory

Many details of the SCF theories used below can be found in the literature.[13,14] Here we will only briefly discuss the main points, focus on the approximations, and mention the parameters that are used. The mathematical details are deferred to the Appendices. In this section we first will discuss the polymer size distribution, pay some attention to the SF-SCF model, and finally discuss the stack of boxes model.

Polymer Length Distribution. A function commonly used to represent polymer molecular weight distributions is the so-called Schulz−Zimm distribution:[15,16]

$$P(x, N_i) = \frac{x^{x+1}}{\Gamma(x+1)} \frac{{N_i}^{x-1}}{{N_n}^{x}} \exp\left(-\frac{xN_i}{N_n}\right) \qquad (1)$$

in which $P(x,N_i)$ is the probability of chains with degree of polymerization N_i, N_n is the number-average degree of polymerization, and x defines the broadness of the distribution. $\Gamma(x+1)$ is the gamma function, which for integer values of x is equal to $x!$. A nice feature of this distribution is that the parameter x is directly related to the polydispersity index:

$$\frac{M_w}{M_n} = \frac{N_w}{N_n} = \frac{x+1}{x} \qquad (2)$$

Here M_n is the number-average molecular weight and M_w is the weight-average molecular weight (both in g/mol). The polydispersity index, M_w/M_n, is the most commonly used measure for polydispersity. The Schulz−Zimm distribution is almost symmetrical at low values of the polydispersity (similar to the Gaussian distribution), but with increasing polydispersity the distribution shifts to a higher frequency of small chains. In this way the distribution can be used to describe very high polydispersities.

Numerical Self-Consistent-Field Theory. We make use of a numerical self-consistent-field (SCF) model with the discretization strategy of Scheutjens and Fleer (SF-SCF). In all calculations an impenetrable surface is present onto which a polymer brush is grafted. The combination of this surface with the brush is called the substrate. Information on the length distribution used for the chains has been given above. The properties of the polydisperse polymer brush have been

discussed at length in ref 14. Here we consider how particles interact with such a brush. The focus is on two limiting cases.

In case *one* we focus on the interaction of small particles with the brush. When the interacting particle is small compared to the relevant properties of the brush, such as the grafting density σ (inverse of the area per molecule) and the chain lengths, one has to account for the fact that the polymer chains can escape from or are attracted toward the space of confinement (the space between the substrate and the interacting particle). Such relaxation effects can be accounted for by using a cylindrical coordinate system (two-gradient SCF). When doing so, it is necessary to compute relevant density gradients perpendicular to the substrate as well as in a radial direction (see Figure 1). In this geometry the particle is modeled as a small cylinder with length L and radius R and has its long axis along the long axis of the coordinate system (see Figure 1 for a schematic illustration).

In case *two* we will consider very large particles interacting with the brush. The radius of the particle is assumed to be much larger than the spacing between the polymer chains and much larger than the length of the polymers. In this limit it is reasonable to ignore the finite size of the interacting particle and consider a polymer brush compressed by a solid wall representing the particle. This problem is conveniently solved using a classical one-gradient SCF model and using a flat geometry.

Generic Aspects of SF-SCF Theory. In general, we are not primarily interested in the conformation of a particular polymer chain in the brush. Instead, the focus is on the average conformations of a large set of polymer chains, resulting, for example, in density profiles. These average conformations can be found by solving the Edwards diffusion equation for the set of polymer chains. Here it is important to mention that for a brush the first segment of each chain is forced to be next to an impenetrable surface S (this is implemented as a constraint). As exact analytical results are not available for this problem, we need some numerical scheme. Details of this scheme are found in the Appendices. Polymer chains with length (degree of polymerization) N_i are referred to by the letter i. The number of chains per unit area of this type, σ_i, are taken from the distribution mentioned above, where the overall grafting density σ is an input parameter. The polymer chains assume non-Gaussian characteristics because they experience a segment potential $u(\mathbf{r})$ (here $\mathbf{r} = (z,r)$ in the case of the two-gradient SCF calculations and $\mathbf{r} = z$ for the one-gradient SCF case). For homopolymers, with united segments A, and grafting density $\sigma > 1/N$, it is well-known that the SF-SCF method predicts a parabolic potential profile $u(z) = A - Bz^2$, in which A and B are constants. In good solvents the volume fraction profile $\varphi(z)$ will then also be parabolic. For polydisperse systems, on the other hand, this is no longer the case. In the segment potential we account primarily for short-range interactions with a monomeric solvent (W). Using the Flory−Huggins parameters, which are dimensionless exchange interaction energies, we limit ourselves to $\chi_{AW} \equiv \chi \leq 0.5$. The (dimensionless) second virial coefficient v is directly linked to the quality of the solvent, i.e., $v = 1 - 2\chi$. The interactions with the solid substrate are taken to be athermal for all components in the system. The interactions with the particle (P) is one of the main parameters that will be varied below. For attraction the adsorption parameter $\chi_P \equiv \chi_{AP} - \chi_{WP} < 0$. For repulsion $\chi_P > 0$. Also included in the segment potential is a Lagrange field $u'(\mathbf{r})$ which assures the incompressibility condition (all lattice sites must either be occupied by polymer segments or solvent molecules or are part of the particle).

Polymers near interfaces experience an entropy loss, simply because the chains cannot penetrate the solid particle P or surface S. In a lattice model the entropy loss is easily estimated. This loss is a function of the a priori probability λ_1 for a segment to go from one layer to a next one. Here we use a (cubic) lattice where $\lambda_1 = 1/6$, and the entropy loss per segment−segment bond next to a flat surface amounts to $\Delta S = k_B \ln(1 - \lambda_1) \approx -k_B\lambda_1$. There exists a critical (dimensionless) adsorption energy χ_P^{cr} below which adsorption takes place and above which the polymers avoid the surface (particle). For a flat surface and for long chains the critical adsorption energy is equal, but opposite, to $T\Delta S/k_BT = \Delta S/k_B$. As a segment next to the surface has λ_1 contacts with the surface, exchange with the solvent gives and energy effect of $\lambda_1\chi_P$. This implies that $\chi_P^{cr} \approx -1$ (recall that the Flory−Huggins parameter is made dimensionless by dividing by k_BT).

The results of the SCF calculations are essentially twofold. On the one hand, there are the measurable volume fraction profiles. These profiles give insight into how the chains accommodate the particle in the brush or deal with the confinement. More importantly for the results, we can evaluate the free energy of interaction. This quantity is computed directly as a function of the volume fraction and the segment potential profiles. Details are given in Appendix A.

Small Particle in Brush: Two-Gradient SCF. We refer once again to Figure 1 where a schematic drawing is given of the calculation "box" for the two-gradient SCF calculations. The use of two gradients allows for the fact that in the case of repulsion the chains that are confined underneath the particle can escape to the unconfined regions and, inversely, in the case of attraction that the chains that are outside the confined region can be drawn toward this space. It then becomes important to decide if the grafting points have a fixed position (quenched) or that the chains can move with the grafting point along the surface (annealed). In the latter case, redistribution of the chains is likely to result in an extra decrease of the free energy.

To check the importance of this effect, we have compared the free energies of interaction between the particle and a bidisperse brush, for mobile chains and fixed chains (evenly distributed along the surface). We found that for a small particle there is only a very small difference between the interaction with the fixed and the mobile brush (for $M_r = 20$). As the annealed grafting condition also solves the issue of which chain lengths to graft in the central region, i.e., near $(z,r) = (1,1)$, we have chosen to model the mobile brush. As long as the particle is far from the surface, each surface site $(1,r)$ has the same probability to have a chain of length N_i grafted to it. Only when the particle is in close proximity of the brush or when it is inserted deep into the brush, the local grafting length distribution may slightly differ from the overall grafting density distribution.

Large Particle in Brush: One-Gradient SCF. In this case a polydisperse brush on a solid surface is confined by a second flat surface, P. Only one relevant coordinate is present in the system, namely the distance z from the substrate surface. When the position $z = D$ of the second surface exceeds the lengths of the longest chains, the brush is unperturbed. This is the reference state for the free energy of interaction. In this case all quantities are normalized per unit surface area, i.e., per lattice site area. As the chains cannot avoid the gap between the particle P and the substrate S, the issue of lateral mobility of the chains does not occur here. Obviously, results from this approach are identical to results that we could get from the two-gradient approach, with a particle that spans the whole box.

"Stack of Alexander−de Gennes Boxes" Model. In ref 14, we proposed an extension of the classical box model to describe polydisperse brushes. In this extension the idea is to use a stack of boxes. The box model is the simplest model for a monodisperse polymer brush as one assumes that all the polymers in the brush have the same stretching and thus that all end points are at the same distance from the grafting interface. This model was first used by Alexander and de Gennes[17,18] and yielded for uncharged polymer brushes simple scaling laws for, e.g., the brush height. In Appendix B we present more details of this model, which can be used to study adsorption of an ensemble of particles into a polymer brush.

A polydisperse brush cannot be described by a model that uses just one single box, as one would need to assume that polymers of different length stretch to the same height, and thus that short chains are extremely extended and long ones are compressed. One can, however, describe a polydisperse brush, in a reasonable fashion, using a stack of boxes. A schematic depiction of this model is shown in Figure 2. The number of boxes equals the number of chain length fractions that is chosen for the modeling (in Figure 2 this number is three). The box directly adjacent to the grafting surface contains all chains. The polymers of the smallest chain length fraction have their end points at the top of this box (at distance H_1 from the surface). As a result, the second box contains polymers of all chain length fractions except the smallest one. The third box contains polymers of all chain length fractions except the smallest two, etc. This continues to the last box which only contains polymers of the longest chain length fraction. Thus, every box has its own local grafting density, which is given by the total number of chains (per unit area) included in that box. Each box also has its own local chain length, which equals the length of the polymers of the smallest chain length fraction in that box, minus the length of the polymers that ended in the box below. In this way, the sum of the chain lengths of all boxes is the length of the longest polymer fraction.

The stack of boxes model (SoB) describes, for a given polymer length distribution, the local grafting density and local chain length for every box. To get more relevant information such as the height, polymer density, or even adsorption in such a box, a local model is needed. The local model gives the local stretching of the chains and evaluates the adsorption of particles onto these chains while both the solvent and the particles can exchange with the bulk. The local model that we use is a box model based on a simple free energy description of a monodisperse brush, combined with a Langmuir-type model to describe adsorption of particles. The idea is that particles adsorb onto sites that are specified along the polymer chains. This is described in detail in Appendix B.

Parameter Settings. In the SF-SCF calculations, we keep the number-average degree of polymerization, the overall grafting density, and the overall mass constant when varying the polydispersity. Unless specified otherwise, we have used the Schulz−Zimm distribution with a maximum chain length of $N_I = 1000$. The overall grafting density σ is fixed at an experimentally relevant value of $\sigma = 0.05$ chains per surface lattice site. (Common experimental values are between 0.01 and 0.3 polymer chains per nm^2.[2−4]) The cylindrical coordinate system has a finite size in the radial direction of $M_r = 20$ and a size of $M_z = 100$ lattice sites above the surface, which is well above the height of the brush. To describe a small particle, we use an object with a radius of $R = 2$ and a height of $L = 3$ lattice sites. We refer to these numbers as ($R \times L$). As the chosen grafting density is 0.05,

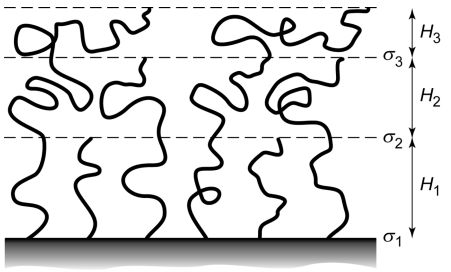

Figure 2. Schematic depiction of a brush in a stack-of-boxes model. Here σ_i represents the grafting density and H_i the height of box i. Small chains reach to height H_1, intermediate chains reach to height $H_1 + H_2$, and the longest chains reach to height $H_1 + H_2 + H_3$. Each layer can be described by a separate box model, with a certain grafting density and chain length, to calculate properties such as the brush height, polymer density, or even the amount of adsorbed particles.

the particle diameter ($2R$) is slightly smaller than the distance between two grafting points ($R \approx 1/(2\sqrt{\sigma})$). To be able to compare the free energy of interaction for the large particle (obtained in the one-gradient coordinate system) with that of the small particle, we multiply the interaction energy obtained for the large particle (which is in k_BT per lattice site) with the surface area of the small particle (thus by πR^2).

The interaction between the particle and polymer segments in the brush is described by the parameter χ_P, and the interaction of the polymer segments with the solvent is given by χ. For this investigation we chose three different sets of values for these parameters. The first set reflects only excluded-volume interactions ($\chi_P = 0$, $\chi = 0$), the second a small attraction between brush and particle in combination with a lower solubility for the polymer chains and the particle ($\chi_P = -1$, $\chi = 0.5$), and the third a strong attraction between brush and particle, also with a lower solubility for the polymer chains and the particle ($\chi_P = -2.5$, $\chi = 0.5$). In the Results and Discussion section, we will more fully discuss this choice of parameters.

For the SoB model we use a brush with $N_n = 100$ and $\sigma = 0.1$. This brush is in contact with a solution containing particles with size respective to the solvent molecules of $N_p = 4$ and a bulk volume fraction of $\Phi_P = 0.001$. The particle size is small compared to the particle used in the SF-SCF model for computational reasons; to compensate, we also use a higher grafting density than in the SF-SCF model. The (reduced) attraction parameter U is varied between $U = 0$ and $U = -5$ to investigate a broad range of attractions. As a rough method to compare the attraction parameter χ_P of the SF-SCF model to the attraction parameter U of the SoB model, we use $U = \chi_P - \chi_P^{cr}$, to which we will come back in the Results and Discussion section.

Results and Discussion

Investigation of Brush and Interaction Parameters. In Figure 3 we show the key prediction of ref 14, namely that the polymer volume fraction profile of a brush is strongly dependent on the polydispersity index. Only for a monodisperse brush the volume fraction profile has an almost parabolic shape: $\varphi(z) \sim \varphi^{max} - Bz^2$, where φ^{max} and B are constants; i.e., it is a concave function. Already for $M_w/M_n = 1.1$ the volume fraction drops almost linearly with the distance to the grafting surface. The profile becomes convex at higher polydispersities. With increasing polydispersity the height above the surface where polymer segments are detected, increases. The average stretching of the chains (not shown) decreases with increasing polydispersity index.

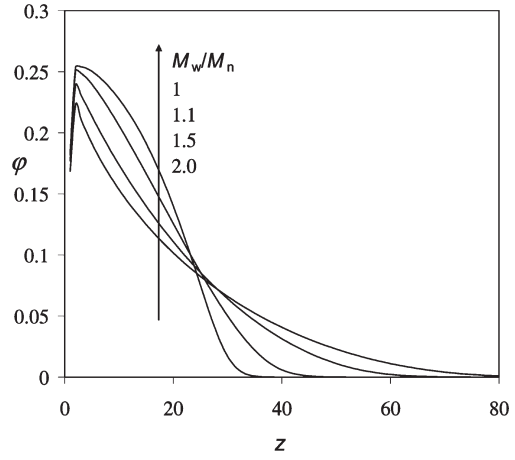

Figure 3. Brush density (φ) as a function of distance from the grafting interface (z) for different polydispersity indices as indicated ($N_n = 100$, $\sigma = 0.05$).

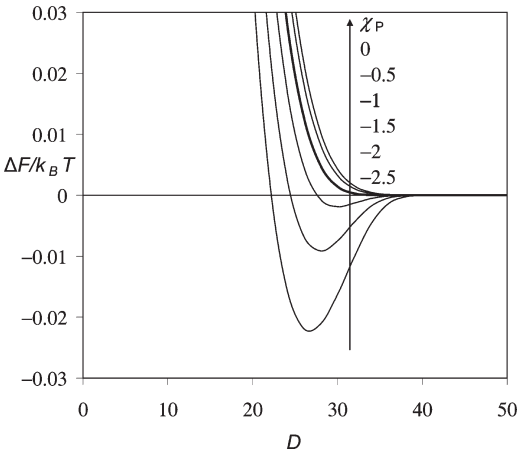

Figure 4. Free energy of interaction (ΔF is given per lattice site) of a large object (a flat wall spanning the whole box) with a polymer brush ($\sigma = 0.05$, $N = 100$) for different values of χ_P as indicated, as a function of distance (D) of the object from the grafting surface as computed using the one-gradient numerical SCF theory. $\chi = 0$.

To investigate the interaction of a polymer brush with a particle, we use the approach by Steels et al.[13] They used the SF-SCF approach in which a single particle is moved from outside the brush to a certain distance from the interface (D) into the brush. The resulting change in free energy is called the free energy of interaction (ΔF). In Figure 4 we show the interaction between a monodisperse brush and a large particle for various values of the polymer−particle interaction strength. This graph clearly illustrates the significance of the critical adsorption energy. At $\chi_P \approx -1$, the entropy loss of the polymer chains touching the particle is matched by the energy gained by adsorption. Thus, above $\chi_P \approx -1$ we only find repulsion, while below $\chi_P \approx -1$ we find attraction for a certain range of D.

We want to investigate the effect that polydispersity has on particle−brush interaction for different values of χ_P. From the results of Figure 4 we have chosen the following three sets interaction parameters. In the first case we want to focus on excluded-volume interactions only, and thus $\chi_P = 0$ and $\chi = 0$. In the second case we investigate a system in which we have a small attraction between the particle and the brush. For this we chose $\chi_P = -1$ and $\chi = 0.5$. In this way the total adsorption energy is slightly more negative than the critical value, and thus a small attraction is expected. In addition, we argue that

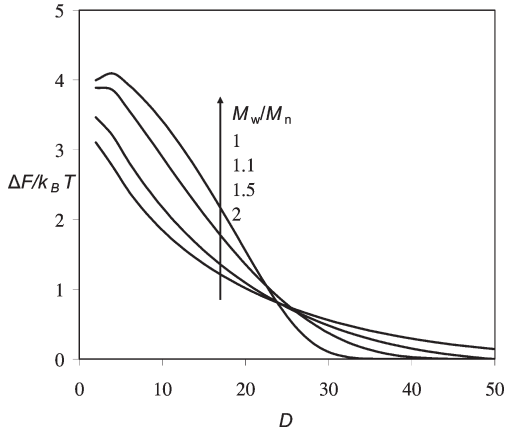

Figure 5. Free energy of interaction (ΔF) of a small object (2×3) in a polymer brush ($\sigma = 0.05$, $N_n = 100$) as a function of distance (D) from the grafting interface, calculated using two-gradient numerical SCF theory ($\chi_P = 0, \chi = 0$).

a reduced solvent quality of the polymer chains ($\chi = 0.5$) is realistic, as a less soluble polymer chain is more likely to be attracted to a particle than a polymer chain in a good solvent. In the third and last case we have chosen $\chi_P = -2.5$ and $\chi = 0.5$, thus leading to a situation where the particle is strongly attracted to the polymer brush.

Interaction of a Polydisperse Brush with a Small Particle. In Figure 5 we show the free energy of interaction between a polymer brush and a small particle (2×3 lattice sites) for different degrees of polydispersity in the first scenario; i.e., the particle has no attractive interactions with the brush. The size of the particle is such that it resembles the interaction of a polymer brush with a small protein. As is observed in Figure 5, at a height of $D > 50$, ΔF is zero (except for the largest polydispersity index), showing that there is no interaction between the brush and the particle. When the particle is moved inside the brush (going to lower distance), the particle comes into contact with the brush and ΔF increases. This repulsion is due to the excluded-volume interactions: when the brush is deformed due to insertion of an object, the brush responds with a restoring force. We observe that the higher the polydispersity index, the further away from the surface nonzero ΔF values are found. This is to be expected as the height of the brush increases with polydispersity. On the other hand, we find that ΔF deeper inside the brush is higher for the monodisperse brush than for the polydisperse brushes. The free energy of interaction depends on the local brush density. As increasing polydispersity leads to an increasing brush height, the brush density near the grafting interface decreases. Because of this lower brush density, ΔF is also lower close to the grafting interface. Thus, the higher the polydispersity, the easier it is for a small particle to penetrate the denser parts of the polymer brush and thus to reach the grafting interface. Polymer brushes are often used as barriers that prevent fouling agents from reaching a surface. The harder it is for the fouling agent to reach the surface, the better the antifouling properties. Hence, we may formulate our first conclusion; namely, that the more monodisperse the brush, the better the antifouling properties against small particles.

Now that we have shown that the polydispersity can influence the antifouling properties of a polymer brush, it is interesting to compare this effect to that of the grafting density. The brush grafting density is commonly seen as the most important parameter for the antifouling properties of a brush.[1−5] The larger the grafting density, the higher the

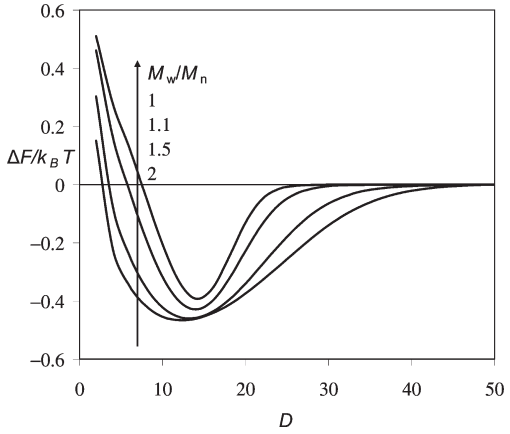

Figure 6. Free energy of interaction of a small object (2×3) in a polymer brush ($\sigma = 0.05$, $N_n = 100$) as a function of distance (D) from the grafting interface, as calculated by two-gradient numerical SCF theory ($\chi_P = -1, \chi = 0.5$).

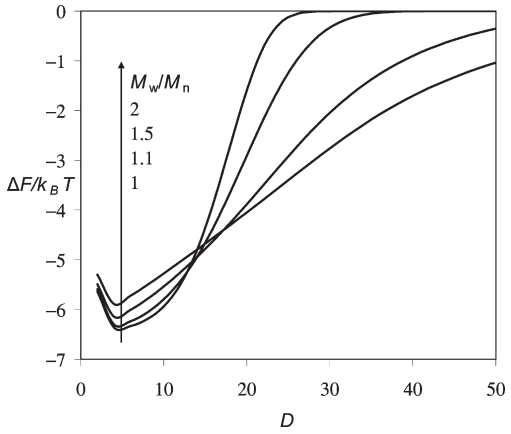

Figure 7. Free energy of interaction of a small object (2×3) in a polymer brush ($\sigma = 0.05$, $N_n = 100$) as a function of distance (D) from the grafting interface, as calculated by two-gradient numerical SCF theory ($\chi_P = -2.5, \chi = 0.5$).

energy barrier that must be overcome by a particle to reach the surface. We calculated, using the parameter settings of Figure 5, the free energy of interaction for a number of different grafting densities (not shown). For a monodisperse brush with $\sigma = 0.1$ we find that the maximum ΔF becomes approximately $8k_BT$, and for $\sigma = 0.2$ we even find a maximum ΔF of approximately $16k_BT$. As the effect of the grafting density on the energy barrier is stronger than the effect of polydispersity, it is clear that the grafting density is the more important tuning parameter for antifouling properties against small particles. Still, for all these grafting densities the maximum ΔF decreases when the polydispersity increases.

In some cases, fouling agents such as proteins have a slight attraction to the polymers in the brush. For such a case, we present in Figure 6 the predictions for the free energy of interaction between a small particle and a polymer brush. As the particle is inserted into the brush, there is an attraction and a minimum in ΔF appears around $D = 14$. Deeper inside the brush the attraction turns into repulsion. This nonmonotonic dependence of ΔF on the position of the particle is a result of the balance between attraction of the polymer chains to the particle and repulsion from the excluded-volume interactions (brush confinement). At low brush densities (at the brush periphery) attraction dominates, but deeper in the brush where the brush density is higher, repulsion dominates. Although the polydispersity hardly effects the depth of the minimum in the free energy, it has a clear effect on the interaction profile. We find that the higher the polydispersity index, the larger the range of D in the brush where attraction is observed. This is due to the fact that for increasing polydispersity the polymer mass is spread over a larger volume, and thus the average brush density decreases. For a broader chain length distribution, the interaction between brush and particle starts further away from the grafting interface, but also the brush density remains low enough for excluded-volume interactions to remain negligible. Only deep in the brush, repulsion due to excluded-volume interactions is dominant. This suggests that, if there is a slight attraction between the brush polymers and, for example, small proteins, the adsorbed amount increases with polydispersity, as there is a larger part of the brush in which attraction dominates. Thus, also if there is a weak attraction between the polymers and the particle, the monodisperse brush is expected to have better antifouling properties than the polydisperse brush.

In Figure 7, we present the free energy of interaction for the case that there is a strong attraction between the particle and the brush. Now, we find that attraction dominates over the whole interaction range. The higher the polydispersity, the further away from the interface (larger D) attraction is found. In Figure 7 the curves cross over between $D = 10$ and $D = 20$: far away from the interface, the attraction is larger for larger polydispersities, while close to the interface, a larger polydispersity results in a less negative ΔF. Thus, the attraction depends on the local brush density, a higher polymer density gives a more negative ΔF. Obviously, such a brush is completely unsuitable for antifouling purposes. Instead, it might be used to store or immobilize particles. Indeed, polymer brushes with strong interaction with proteins have been investigated for their use as protein carriers.[20,21] Note that here we only consider the case of an isolated particle in the brush. When many particles are simultaneously allowed to adsorb into the brush, one can anticipate that this would lead to strong changes in the density profile of the brush (such as swelling of the brush due to the insertion of the extra volume or a collapse of the brush due to strong attraction between the polymer chains and the particles). If there is a strong attraction between polymer and protein, one would not expect a large effect of the polydispersity on the adsorbed amount. This quantity will depend mainly on the total amount of polymer in the brush and not so much on the way that it is distributed.

As stated before, the problem of adsorption of many particles is currently out of reach for molecularly realistic SF-SCF models. We can, however, use the results of our model to predict the adsorption for low bulk particle concentration. In this regime (the so-called Henry regime) the adsorption is considered to be so low that the brush is unperturbed by this adsorption. This implies that the particle density in the brush, φ_p, is only determined by the bulk volume fraction of particles, Φ_p, and the energy of interaction:

$$\varphi_p(D) = \Phi_p \exp\left(\frac{-\Delta F(D)}{k_B T}\right) \quad (3)$$

Using eq 3, we thus find that the particle profile inside the brush is not homogeneous. For example, close to the surface there may be a depletion of particles with respect to the bulk value, whereas on the brush periphery the adsorption is positive (Figure 6). Clearly, for a polydisperse brush there is a larger region with positive adsorption of particles compared to the monodisperse brush (Figures 6 and 7).

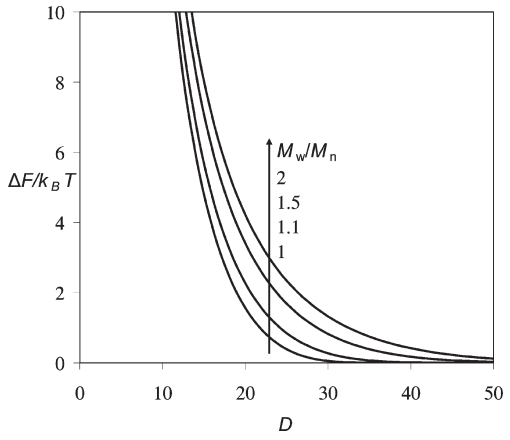

Figure 8. Free energy of interaction (ΔF) of a large object (a flat wall spanning the whole box) on a polymer brush ($\sigma = 0.05$, $N = 100$) as a function of distance (D) from the grafting interface, as calculated by one-gradient numerical SCF ($\chi_P = 0$, $\chi = 0$). For comparison with Figure 5, ΔF has been multiplied by lower surface area of the small particle (4π).

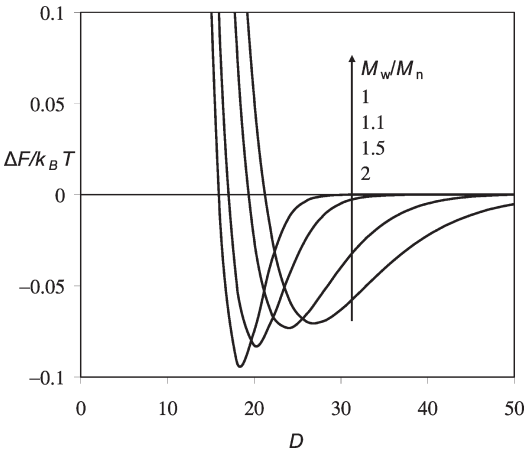

Figure 9. Free energy of interaction of a large object on a polymer brush ($\sigma = 0.05$, $N_n = 100$) as a function of distance (D) from the grafting interface, as calculated by one-gradient numerical SCF theory ($\chi_P = -1$, $\chi = 0.5$).

Interaction of a Polydisperse Brush with a Large Particle. As stated earlier, there is large difference between a small particle and a large particle interacting with a brush. A small particle (such as a globular protein) can easily penetrate a brush, as the brush polymers can surround the particle. Thus, interaction with the particle in the polymer brush mainly depends on the local brush density. A large particle (such as a bacterium or a colloidal probe for atomic force microscopy (AFM)) cannot penetrate into a brush; it can only compress it. To investigate the interaction of a polydisperse brush with a large particle, we replaced the latter by a flat hard wall. Just as with the small particle, this wall is moved from far above the brush to a distance D from the grafting interface, and the difference in free energy is calculated. In Figure 8 results of such calculations are shown. The free energy of interaction is normalized to the surface area of the small particle to facilitate comparison. In Figure 8 only excluded-volume interactions are taken into account (compare with Figure 5). As can be seen, the interaction energy shows a very strong increase when the particle approaches the grafting interface. The closer the particle wall comes to the grafting surface, the more the polymer brush is compressed. The interaction energy is much larger than for a small particle, simply because the chains cannot escape from the confined region. Polydispersity has a large influence on the interaction energy: at every height we find that the higher the polydispersity, the higher the interaction energy. In other words, it is harder to compress a polydisperse brush than a monodisperse brush. Thus, for the case that there is no attraction between the brush chains and the particles, polydispersity helps to prevent adsorption of large particles (e.g., when there is some long-range interaction between the interface and the particle).

At this stage it is useful to explain why a polydisperse brush is harder to compress than a monodisperse brush. De Vos and Leermakers[14] found for an unperturbed brush that with increasing polydispersity there is more freedom (compared to a monodisperse brush) to distribute the stretching of the chains. One consequence of this is that the average stretching (defined as the height increase per monomer) is lower for a polydisperse brush than for a monodisperse brush. For example, the average stretching of a brush with a polydispersity $M_w/M_n = 2$ was found to be 22% lower than that of a monodisperse brush. The relevance for compression of the brush is evident. The entropy loss as a result of compression is higher for a polydisperse brush. This results in a higher free energy of interaction for the polydisperse brush with a large object than for the monodisperse brush.

In Figure 9 we examine the case in which there is a small attraction between the large particle and the chains in the polymer brush. Similar to Figure 6, which shows comparable results for a small particle, we observe an attraction between brush and particle in the region where the brush density is low. Also, with increasing compression of the brush the repulsion ultimately exceeds the attraction. Again, this behavior is the result of a balance of forces: the closer the particle is moved to the grafting interface the higher the compression, but also, up to saturation, the higher the number of possible contacts between brush polymers and the particle. This results in a minimum of ΔF as a function of D. The polydispersity determines the position and depth of this minimum. With increasing polydispersity, the minimum moves further away from the grafting interface and the depth of the minimum slightly decreases. A more significant effect of polydispersity, however, is the change in the range of D where we find attraction between the brush and the particle. We find that the higher the polydispersity, the larger this range.

The same effect of polydispersity is observed in Figure 10, which shows the interaction energy between the large object and the brush when there is a strong attraction ($\chi_P = -2.5$). Because of this strong attraction, the minima in the free energy are much larger than in Figure 9, but the trend is the same: an increase in polydispersity leads to a shift of the minimum in the free energy further away from the grafting interface, and the depth of this minimum slightly decreases. A more pronounced effect is that the range of D in which attraction is found increases with increasing polydispersity. As was observed in Figure 8, repulsion due to compression increases with increasing polydispersity. Therefore, the monodisperse brush can be compressed more than the polydisperse brushes, resulting in more contacts between the brush and the particle and thus a slightly deeper free energy minimum at a lower height. Although this effect is not so large, it does show that for the protection of a surface against fouling by large particles a polydisperse brush is the better choice.

Experimentally, the role of polydispersity in the interaction of particles with a brush has not yet been addressed.

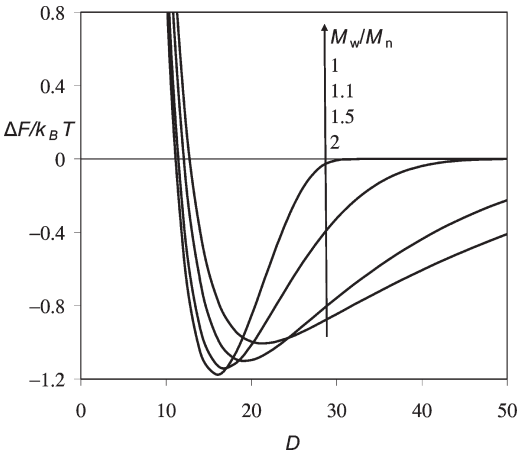

Figure 10. Free energy of interaction of a large object on a polymer brush ($\sigma = 0.05$, $N_n = 100$) as a function of distance (D) from the grafting interface, as calculated by one-gradient numerical SCF theory ($\chi_P = -2.5$, $\chi = 0.5$).

Colloidal probe AFM is potentially suited to measure the interaction between a large particle and a polymer brush and could thus be used to verify some of our predictions. As an alternative one could use the surface force apparatus (SFA) to measure the interaction between a polymer brush and a planar surface or between two polymer brushes. For such experiments, however, it is necessary that one has a method to produce polymer brushes with different polydispersities while N and σ are retained.

Adsorption of Many Particles in the Polydisperse Brush. In Figures 5−7 it was shown that the interaction energy between a brush and a single small particle is influenced by polydispersity. Therefore, it is also interesting to investigate how the interaction with many particles depends on the polydispersity. We will now focus on the adsorbed amount of particles in the brush and how this depends on the polydispersity. This is of relevance as adsorption of small particles to a brush (in this context called secondary adsorption) is a problem for its antifouling properties but also because polymer brushes may be employed to accommodate or immobilize particles (such as proteins, especially enzymes) rather than prevent fouling.[20,21]

As explained in the Theory section, we use an elaborate box model to quantify particle adsorption into a polydisperse brush (see also Appendix B). A similar, but slightly different, box model has been advanced before to study adsorption into a polymer brush, and qualitative agreement with experimental results was reported.[8] Here, the focus is on a polydisperse brush. This feature is implemented by using not a single box but rather a stack of boxes (SoB) to describe the brush. Even though such a SoB model does not accurately describe the brush density profile for a given polydispersity, it reasonably well describes the trends observed for brush density profiles as a function of polydispersity (as shown in Figure 3).

To be able to compare the outcome of the SoB model with the results of the SCF calculations, it is helpful to explain the relation between the SoB model interaction parameter U and the SCF interaction parameter χ_P. We have already discussed that for low particle concentrations the adsorption can be directly calculated from ΔF (eq 3). Here ΔF is the result of a balance between the attraction between particle and polymer segments on the one hand and the excluded volume interactions on the other. In the SoB model the adsorption is the result of exactly the same

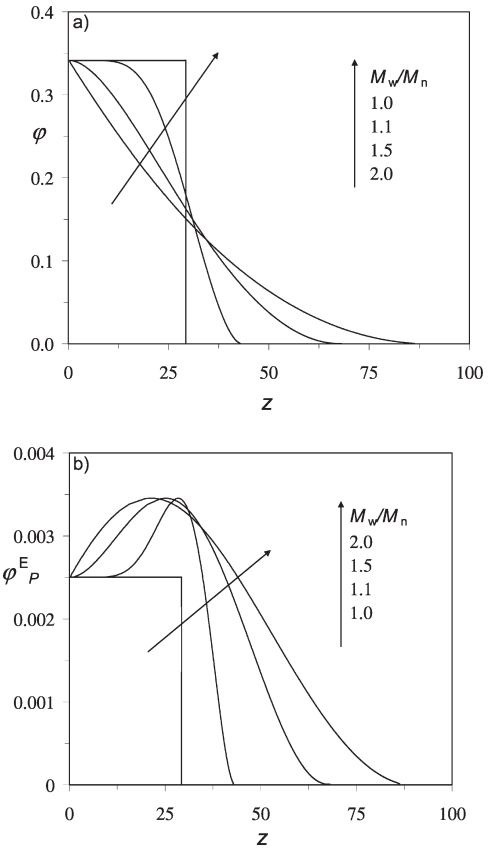

Figure 11. Density profile of a polymer brush ($\sigma = 0.1$, $N_n = 100$) in contact with a particle solution ($N_P = 4$, $U = -1$, $\Phi_P = 0.001$) for different polydispersities as indicated, calculated with the SoB model. (a) Polymer density (φ). (b) Excess particle density ($\varphi^E_P = \varphi_P + \alpha\varphi - \Phi_P$).

balance of interactions. For the SCF model, it is only above the critical adsorption energy ($\chi_P^{cr} \approx -1$) that ΔF can become negative (see Figure 4) at low polymer densities. In the SoB model we do not take into account the entropy loss of the polymer chain upon contact with a particle, and thus the interaction energy can become positive at low polymer densities for $U > 0$. Hence, we can propose that $U = \chi_P - \chi_P^{cr}$ as a first-order approximation.

In Figure 11, we show results of the SoB model for the specific case of a brush ($\sigma = 0.1$, $N_n = 100$) in contact with a particle solution ($N_P = 4$, $U = -1$, $\Phi_P = 0.001$). In Figure 11a we present the polymer density profile for a number of polydispersities. Comparison with Figure 3 proves that the SoB model reproduces trends of the more detailed SF-SCF model: there is a clear increase in brush height and the change of the profile evolves toward the convex shape with increasing polydispersity indices. In Figure 11b we give the corresponding excess particle density profile that results from the adsorption of the particles inside the brush. Clearly, the differences in the polymer density profiles for the different polydispersities lead to large variations in the particle uptake into the brush. For the monodisperse brush (as described by the SoB model), the polymer density is equal throughout the whole brush, and thus the particle density is also equal throughout the brush. However, for polydisperse brushes there is a maximum in the particle density at a certain height in the brush. The higher the polydispersity, the broader this maximum. It results from the nonmonotonic relation between the particle density and the polymer segment density in the brush. For low polymer densities, the adsorption increases because the number of binding sites increases. At

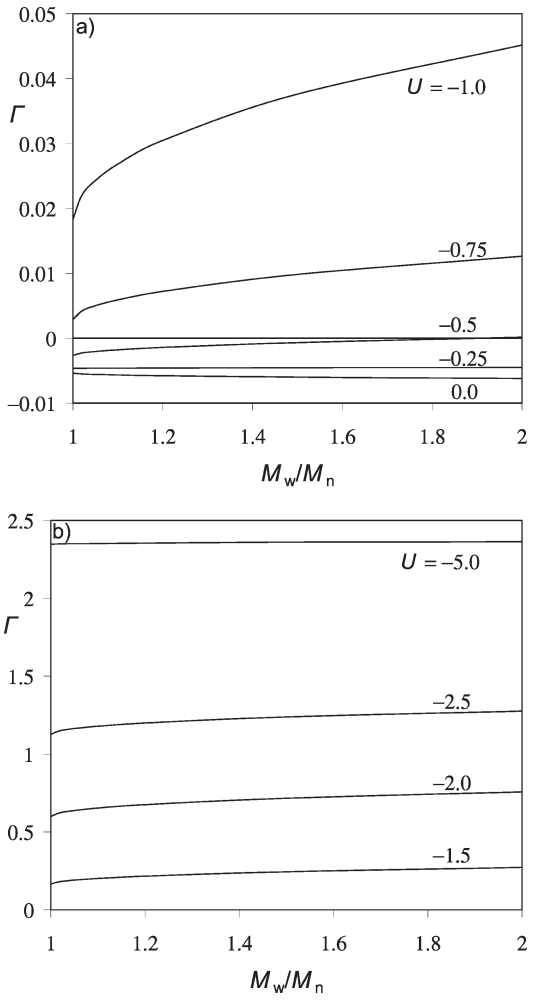

Figure 12. Adsorbed amount (Γ), in number of particles per surface area, of small particles ($N_p = 4$, $\Phi_P = 0.001$) in a polymer brush ($N_n = 100$, $\sigma = 0.1$) as a function of polydispersity and for a number of different adsorption energies (U) as indicated. Calculated with the stack of boxes model. (a) Low U values. (b) High U values.

higher polymer densities, however, the adsorption levels off due to volume exclusion. Both of these effects have already been discussed in the context of the SF-SCF calculations. Indeed, the single-particle insertion model has a relevance for the adsorption profile.

It is expected that the changes in the density profiles of the particles as a function of polydispersity will also lead to changes in the total adsorbed amount. In Figure 12 we show the adsorbed amount as a function of the polydispersity index for a number of adsorption energies. The adsorbed amount is defined here as the excess (more than the bulk concentration) number of particles per surface lattice site. For the lowest adsorption energies (Figure 12a, $U = 0$, $U = -0.25$), the adsorption is negative. Thus, the density of particles is lower in the brush than it is in bulk solution. This is due to the excluded volume effects of the brush. As a function of polydispersity the negative adsorption remains fairly constant. Interestingly, this is different for the somewhat higher adsorption energies ($U = -0.5$, -0.75, and -1.0). In the case that $U = -0.5$, the negative adsorption at low polydispersities turns into positive adsorption at high polydispersities. Admittedly, in the absolute sense there is just a little change in binding, but the switch in sign is of interest from a theoretical point of view. In the case that $U = -0.75$ or -1.0, the adsorption is low for all polydispersity indices, but the relative changes are large; i.e., over the range $M_w/M_n = 1-2$ the adsorption changes by a factor of respectively 4.4 and 2.5. This increase can be well understood by considering the results of Figure 11. The interaction between brush and particle is so weak that the particles are pushed out of the denser region of the brush. This is very similar to the observations made in Figure 6 where we found that, for a small attraction between brush and particle, attraction is only found in the outer part of the brush where the polymer density is not so high. For the polydisperse brush, the brush density is spread out over a larger height, thus increasing the volume where we find a net attraction between the brush and the particle, which results in larger adsorbed amounts.

At higher (more negative) values for U (Figure 11b) we find that the polydispersity has only a limited effect on the adsorption. The increase in adsorption between $M_w/M_n = 1$ and 2 changes from about 60% for $U = -1.5$ to only about 1% for $U = -5$. For these high adsorption energies, there is only a very limited effect of the excluded-volume interactions. Therefore, adsorption does not really depend anymore on how the polymer is distributed in the brush, but mainly on the amount of available adsorption sites (hence total amount of polymer in the brush).

In this investigation, we have kept the input parameters of the box model relatively simple. It should be noted that with the same method it is possible to do more system-specific investigations. For example, the effect of solvent quality can be investigated by adding an interaction parameter to describe the interaction between solvent and polymers. The effect of charge can be investigated by using a (salt dependent) interaction parameter to describe repulsion between the particles (as has been done in ref 8). In addition, it is possible to introduce an interaction parameter that describes interaction between polymer segments. By changing that parameter upon adsorption of a particle to attraction, it is possible that the brush collapses due to particle adsorption.

Conclusions

Using a numerical self-consistent-field approach, we have investigated the effects of polydispersity of a polymer brush on its interaction with particles. It is found that with increasing polydispersity it becomes easier for a small particle ($R = 1/(2\sqrt{\sigma})$, size comparable to a globular protein) to penetrate into the brush. When there is a small attraction between the particle and the polymer segments, we find that the particle has a net attraction to the brush only if the brush density is not too high. Since with increasing polydispersity the polymer chains are distributed over a large volume (lowering the average brush density), the particle is able to adsorb in a much larger part of the brush. From this we can conclude that a monodisperse brush is better suited to protect an interface against the adsorption of small particles than a polydisperse one. Still, when we compare this effect of polydispersity to the effect of the brush grafting density on brush particle interactions, we find that the grafting density is the more important parameter for tuning the antifouling properties of a brush.

The effect of polydispersity is very different for a large particle ($R \rightarrow \infty$, comparable to an AFM colloidal probe or bacteria). We find that it is harder to compress a polydisperse brush than a monodisperse one. As the polydisperse brush can distribute its segments over a larger volume compared to the monodisperse brush, compression of such a brush results in a larger loss of entropy and thus more resistance against compression. This also means that when there is an attraction between the particle and the polymer segments, the most

favorable interaction is found for the monodisperse brush. The found differences in this interaction are, however, only small. From the above we predict that a polydisperse brush is more suited to prevent the adsorption of large particles to an interface. This prediction might well be tested with SFA or AFM force measurements if one would be able to prepare a set of polymer brushes differing only in polydispersity.

A complementary model, which involves an extension of the Alexander−de Gennes box model toward the stacking of boxes, is used to calculate the total adsorbed amount of small particles to a polymer brush as a function of polydispersity. For a weak attraction between polymer chains and particles, the adsorbed amount increases relatively strong with increased polydispersity, although the absolute adsorbed amount remains low. This again leads to the conclusion that monodisperse polymer brushes are better suited to prevent the adsorption of small particles than corresponding polydisperse brushes. For strong attraction between particles and polymer the effect of polydispersity on the adsorbed amount is very limited as the dominating factor in the adsorption becomes the total amount of polymer (the number of adsorption sites) and not the way in which the polymer is distributed.

Acknowledgment. We thank Unilever Research, Port Sunlight, UK, for encouragement and funding.

Appendix A. SF-SCF Model for Polydisperse Brushes in One- and Two-Gradient Applications

In the present systems we reserve $i=0$ to refer to the monomeric solvent (segment type W), while $i = 1, 2, ..., I$ refers to polymer chains of different length, where chain i has length N_i. The grafting surface is denoted by the letter S and the particle by P. For a given SCF calculation the positions of S and P are fully specified and fixed. In the coordinate system $\mathbf{r}=(z,r)$ (see Figure 1) we thus have fixed the volume fractions of both S and P to unity at coordinates where the surface and the particle exists and zero otherwise. The remainder of the sites $\mathbf{r} = \mathbf{r}'$ is available for the solvent molecules and the polymers segments.

Basically, in the SCF method the free energy F (more specifically, the Helmholtz energy) is optimized. This free energy can be expressed as a function of the volume fraction and potential profiles. The solvent is the only component that is in equilibrium with a reservoir. For this problem the relevant thermodynamic potential is given by

$$F^{\mathrm{po}} = F - n_{\mathrm{W}}\mu_{\mathrm{W}} \tag{A1}$$

where n_{W} is the number of solvent molecules and μ_{W} the corresponding chemical potential, and F^{po} is the partial open free energy. As in the bulk, i.e., far above the brush, the volume fraction of solvent is unity; the chemical potential of the solvent can conveniently be fixed to zero when we assume incompressibility (see also Lifshitz et al.[22]), hence $F^{\mathrm{po}} = F$. Now, the free energy of a polydisperse brush is given by

$$\frac{F}{kT} = -\sum_{i>0}\sigma_i \ln Q_i - \sum_{\mathbf{r}'}\varphi(\mathbf{r})u(\mathbf{r}) - \sum_{\mathbf{r}'}\varphi_{\mathrm{W}}(\mathbf{r})u_{\mathrm{W}}(\mathbf{r}) + \sum_{\mathbf{r}'}[\varphi(\mathbf{r}')\chi\langle\varphi_{\mathrm{W}}(\mathbf{r}')\rangle + \varphi(\mathbf{r}')\chi_{\mathrm{P}}\langle\varphi_{\mathrm{P}}(\mathbf{r}')\rangle] \tag{A2}$$

In this equation Q_i is the single-chain partition function, which can be computed once the segment potentials are known (i.e., the result of the propagator procedure discussed briefly below). In eq A2 the angular brackets imply a local averaging of the quantity over all neighboring lattice sites weighted by the a priori step probabilities to move to such site (which depend on the geometry). Note that there is a constraint imposed on eq A2 that at all coordinates

$$\varphi+\varphi_{\mathrm{W}} = 1 \tag{A3}$$

Optimization of the free energy (eq A2) with this constraint leads to the well-known self-consistent-field equations, which may be expressed by

$$u[\varphi(\mathbf{r})] \rightleftharpoons \varphi[u(\mathbf{r})] \tag{A4}$$

In other words, this equation says that the segment potentials are found from the volume fraction profiles (left-hand side of eq A4) and the segment volume fractions are computed from the segment potentials (right-hand side of eq A4). For the mathematical details we refer to the literature.[14,19] Here it suffices to mention that for given segment potentials there exists an efficient propagator scheme to compute the single-chain partition functions on the one hand and the volume fraction profile for polydisperse brushes on the other hand. This propagator scheme implements a Markov approximation for the polymer chains (freely jointed chain model). It evaluates the statistical weights of all possible and allowed chain conformations and sums the result properly. In the segment potentials the short-range interactions are parameterized by Flory−Huggins parameters and the use of local volume fractions implies the Bragg−Williams mean-field approximation.

The optimal free energy (eq A2), that is, the self-consistent-field solution or the fixed point of eq A4, is found numerically with a precision of at least 7 significant digits. It is clear that this free energy is a function of the distance of the particle from the surface, i.e., $F = F(D)$. The free energy of interaction is found by subtracting the value of the free energy for very large distance of the particle from the surface, i.e.

$$F^{\mathrm{int}}(D) = F(D) - F(\infty) \tag{A5}$$

These calculations can be done for a two-gradient geometry. In this case the interaction free energy directly represents the work needed to insert the particle to a position D. Alternatively, when we consider a large particle interacting with the brush, we use one-gradient SCF calculations. Usually, the free energy of interaction is then normalized per unit surface area, i.e., per area of a lattice site. However, in this paper we have multiplied this by the cross-section area of the small particle πR^2 for ease of comparison of the one-gradient SCF with the two-gradient SCF calculations.

Appendix B. A Quasi-Analytical Box Model for Adsorption

A stack-of-boxes theory has been used to describe the adsorption of particles in a polydisperse brush. This theory requires as input a description of each individual box. The submodel that gives this information is discussed here. In this submodel we do not have to worry about polydispersity, since in each box all chains are equally long, having N segments. The grafting density is σ. We assume athermal interactions except for the interaction parameter between the particles and the polymer. For each contact (and exchange with the a solvent molecule) this interaction energy is given by U (in units of $k_{\mathrm{B}}T$). Here we assume, according to the quasi-chemical approach, either that a particle is fully adsorbed (all particle segments in contact with a polymer segment) or that the particle is not adsorbed (no contact with polymer segments). The particles adsorb onto the polymer chains in a Langmuir-type way. Hence, the maximum adsorption is linked to the total amount of polymer per unit area. We do not take into account any adsorption of particles on the surface. Besides the adsorption energy U, the grafting density σ, and the chain length N, the volume fraction of particles in the bulk Φ_{p} is an input quantity. Typically, in a Langmuir model one assumes that the solvent molecule is of the same size as the adsorbing species. Here we take a slightly more general model and allow for

a size ratio given by N_p (which is the number of times that the particle is larger than the solvent). The outcome of the calculations is the brush height H, the amount of particle segments per unit area θ, and, related to this, the adsorption Γ. There are two incompressibility constraints. In the bulk the volume fraction of particles and solvent must add up to unity:

$$\Phi_p+\Phi_s = 1 \tag{B1}$$

and in the brush we have

$$\frac{\theta}{H}+\varphi_s+\varphi = 1 \tag{B2}$$

where $\varphi = \sigma N/H$ is the volume fraction of polymer in the box.

The starting point for the box model is the free energy G per chain (in units of k_BT).

$$G = F^{\text{elastic}}+F^{\text{adsorption}}+F^{\text{mixing}} \tag{B3}$$

The first term in eq B3 gives the dimensionless free energy of stretching of the polymer chains in the brush. Here we use the Gaussian chain model and write

$$F^{\text{elastic}} = \frac{3}{2}\frac{H^2}{N} \tag{B4}$$

The second contribution to the free energy stems from the adsorption process. Here we introduce the fraction α of polymer covered by the particles. The fraction of polymer in contact with the solvent is thus given by $1 - \alpha$. The total dimensionless adsorption energy per polymer chain for a given fractional coverage is given by

$$F^{\text{adsorption}} = \alpha UN \tag{B5}$$

Hence, the maximum adsorption energy is found for $\alpha = 1$ and this is limited by the total amount of polymer in the brush.

In the box model we need to account for the dimensionless mixing entropy. In this model we have two contributions: one related to the adsorption process and the other related to the exchange of particles an solvent with the bulk.

$$F^{\text{mixing}} = N\left[\frac{\alpha}{N_p}\ln\frac{\alpha}{\varphi_p}+(1-\alpha)\ln\frac{1-\alpha}{1-\varphi_p}\right]+ \frac{H}{\sigma}\left[\frac{\varphi_p}{N_p}\ln\frac{\varphi_p}{\Phi_p}+\varphi_s\ln\frac{\varphi_s}{\Phi_s}\right] \tag{B6}$$

The first part of this equation describes the mixing entropy along the polymer chain, it is multiplied by N to give the free energy per polymer chain. The second term describes the exchange of the solvent and particles in bulk, with solvent and free (unadsorbed) particles in the polymer brush. The free particle volume fraction in the brush is given by φ_p This second term is multiplied by H/σ, which gives the volume of the brush per polymer chain.

Optimization of the total free energy (eq B3) with respect α gives a Langmuir-type equation:

$$\frac{\alpha}{(1-\alpha)^{N_p}} = \frac{\varphi_p}{(1-\varphi_p)^{N_p}}e^{-UN_p} \tag{B7}$$

which specifies the relation between α and φ_p. Similarly, there exists a relation between bulk volume fractions and corresponding quantities in the brush for those components that are free to exchange. Here the size ratio between solvent and particles appears as well

$$\frac{\varphi_p}{\Phi_p} = \left(\frac{\varphi_s}{\Phi_s}\right)^{N_p} \tag{B8}$$

Equation B8 thus shows that the volume fractions of φ_p and φ_s are coupled.

Next, we need to optimize the free energy G with respect to H. We do this numerically, in short as follows. For a given value of H, we know the volume fraction of polymer φ. Using the compressibility relations (B1 and B2), we are left with two equations (B7 and B8) with two unknowns, namely α and φ_s. After solving these equations, we can evaluate G. We continue changing H until G is optimized. This is routinely done up to 5 significant digits.

The excess particle density is found by

$$\varphi_p^E = \varphi_p+\alpha\varphi-\Phi_p \tag{B9}$$

while the excess adsorbed amount (in particles per surface area) is found by

$$\Gamma = \frac{H\varphi_p^E}{N_p} \tag{B10}$$

References and Notes

(1) Milner, S. T. *Science* **1991**, *251*, 905.
(2) Currie, E. P. K.; Norde, W.; Cohen Stuart, M. A. *Adv. Colloid Interface Sci.* **2003**, *100−102*, 205.
(3) Zhao, B.; Brittain, W. J. *Prog. Polym. Sci.* **2000**, *25*, 677.
(4) Advincula, R. C.; Brittain, W. J.; Caster, K. C.; Rühe, J., Eds. *Polymer Brushes. Synthesis, Characterization, Applications*; Wiley-VHC: Weinheim, 2004, ISBN 3-527-31033-9.
(5) Halperin, A. Leckband, D. E. *C. R. Acad. Sci. Paris* **2000**, Series *IV*, 1171.
(6) Mori, Y.; Nagaoka, S.; Takiuchi, H.; Kikuchi, T.; Noguchi, N.; Tanzawa, H.; Noishiki, Y. *Trans.—Am. Soc. Artif. Intern. Organs* **1982**, *28*, 459.
(7) Efremova, N. V.; Sheth, S. R.; Leckband, D. E. *Langmuir* **2001**, *17*, 7628.
(8) Currie, E. P. K.; van der Gucht, J.; Borisov, O. V.; Cohen Stuart, M. A. *Pure Appl. Chem.* **1999**, *71*, 1227.
(9) McPherson, T.; Kidane, A.; Szleifer, I.; Park, K. *Langmuir* **1998**, *14*, 176.
(10) Jeon, S. I.; Lee, J. H.; Andrade, J. D.; DeGennes, P. G. *J. Colloid Interface Sci.* **1991**, *142*, 149.
(11) Szleifer, I.; Carignano, M. A. *Macromol. Rapid Commun.* **2000**, *21*, 423.
(12) Halperin, A.; Fragneto, G.; Schollier, A.; Sferrazza, M. *Langmuir* **2007**, *23*, 10603.
(13) Steels, B. M.; Koska, J.; Haynes, C. A. *J. Chromatogr., B* **2000**, *743*, 41.
(14) de Vos, W. M.; Leermakers, F. A. M. *Polymer* **2009**, *50*, 305.
(15) Schulz, G. V. *Z. Phys. Chem. (Munich)* **1939**, B43.
(16) Zimm, B. H. *J. Chem. Phys.* **1948**, *16*, 1099.
(17) Alexander, S. *J. Phys. (Paris)* **1977**, *38*, 983.
(18) DeGennes, P. G. *J. Phys. (Paris)* **1976**, *37*, 1443.
(19) Roefs, S. P. F. M.; Scheutjens, J. M. H. M.; Leermakers, F. A. M. *Macromolecules* **1994**, *27*, 4810.
(20) Wittemann, A.; Ballauff, M. *Phys. Chem. Chem. Phys.* **2006**, *8*, 5269–5275.
(21) de Vos, W. M.; Biesheuvel, P. M.; de Keizer, A.; Kleijn, J. M.; Cohen Stuart, M. A. *Langmuir* **2008**, *24*, 6575–6584.
(22) Lifshitz, I. M.; Grosberg, A.Yu.; Khokhlov, A. R. *Rev. Mod. Phys* **1978**, *50*, 683.